

Dependence of the Gold Nanorod Aspect Ratio on the Nature of the Directing Surfactant in Aqueous Solution

Jinxin Gao,[†] Christopher M. Bender,[‡] and Catherine J. Murphy^{*,†}

Department of Chemistry and Biochemistry, University of South Carolina, 631 Sumter Street, Columbia, South Carolina 29208, and Division of Natural Sciences and Engineering, University of South Carolina—Spartanburg, 800 University Way, Spartanburg, South Carolina 29303

Received May 27, 2003. In Final Form: August 8, 2003

A three-step seed-mediated growth method was used to make gold nanoparticles. Different surfactants, alkyltrimethylammonium bromides (C_n TAB, $n = 10, 12, 14, 16,$ and 18) and cetylpyridinium chloride (C_{16} PC), were chosen as stabilizers. In general, it was found that as the length of the surfactant chain increased, the resulting gold nanoparticles' aspect ratio increased: the aspect ratio was 1 (for C_{10} TAB), 5 ± 2 (C_{12} TAB), 17 ± 3 (C_{14} TAB), and 23 ± 4 (C_{16} TAB). The plasmon absorption maxima for the gold nanoparticles varied as a function of the shape, from 520 nm (spheres) to beyond 2000 nm (high aspect ratio nanorods). We propose that the surfactant binds as a bilayer to the growing nanoparticle and assists in nanoparticle elongation via a "zipping" mechanism.

Introduction

There is a great deal of current interest in the synthesis of anisotropic inorganic nanomaterials, especially nanorods and nanowires, for potential applications in information technology, optoelectronics, and sensing.^{1–8} Our group^{5,9–13} and others^{14–18} have been active in developing solution-based routes to these materials. In particular, our group has developed a seed-mediated growth approach to making gold and silver nanorods in aqueous solution, with the surfactant cetyltrimethylammonium bromide (C_{16} TAB) as the directing agent^{5,9–13} to produce rods over spheres. The growth of gold nanorods in our

case appears to be governed by preferential adsorption of C_{16} TAB to different crystal faces during the growth, rather than by C_{16} TAB functioning as a soft micellar template.¹³ Other workers have shown that C_{16} TAB adsorbs to gold nanorods in a bilayer fashion, with the trimethylammonium headgroup of the first monolayer of C_{16} TAB facing the gold surface.¹⁹ In our proposed growth mechanism, we envision that the C_{16} TAB headgroup would bind better to the {100} faces of gold that exist along the length of the pentahedrally twinned rods¹³ compared to the {111} gold faces that are at the ends of the rods, as a result of epitaxy.¹³ If this is indeed the primary driving force for growth of gold nanoparticles into nanorods, then simple tetraalkylammonium salts may also yield gold nanorods in our preparation procedures.

In this paper, we examine the dependence of the gold nanorod product shape as the nature of the surfactant is varied. We examined C_{16} TAB analogues in which the length of the hydrocarbon tail was varied, keeping the headgroup and counterion constant, and also an example in which the tail length was kept the same, but the headgroup and counterion both varied. We find, surprisingly, that the length of the surfactant tail is critical for producing gold nanorods. We propose a "zipping" mechanism to account for our results, in which the van der Waals stabilization of the surfactant bilayer on the gold surface due to interchain packing assists the underlying nanorod formation.

Experimental Section

Materials. Hydrogen tetrachloroaurate(III) trihydrate ($\text{HAuCl}_4 \cdot 3\text{H}_2\text{O}$, 99.9+%), trisodium citrate dihydrate (99%), sodium borohydride (NaBH_4 , 99%), and L-ascorbic acid (99+%) were all purchased from Aldrich. Decyltrimethylammonium bromide (C_{10} TAB, 98%) was obtained from Fluka, while the remaining surfactants dodecyltrimethylammonium bromide (C_{12} TAB, 99%), myristyltrimethylammonium bromide (C_{14} TAB, 99%), C_{16} TAB (99%), octadecyltrimethylammonium bromide (C_{18} TAB), and cetylpyridinium chloride monohydrate (C_{16} PC, 98%) were obtained from Aldrich (Table 1). All chemicals were used as received. The C_n TAB surfactants for $n = 10, 12,$ and 14 were freely soluble in water at room temperature. To achieve the required concentrations of C_{16} TAB, the C_{16} TAB solution (if precipitate was observed) was heated to 50 °C, allowed to cool

* To whom correspondence should be addressed. E-mail: murphy@mail.chem.sc.edu.

[†] Department of Chemistry and Biochemistry, University of South Carolina.

[‡] Division of Natural Sciences and Engineering, University of South Carolina—Spartanburg.

- (1) Hu, J.; Odom, T. W.; Lieber, C. M. *Acc. Chem. Res.* **1999**, *32*, 435.
- (2) El-Sayed, M. A. *Acc. Chem. Res.* **2001**, *34*, 257.
- (3) Huang, M. H.; Mao, S.; Feick, H.; Yan, H.; Wu, Y.; Kind, H.; Weber, E.; Russo, R.; Yang, P. *Science* **2001**, *292*, 1897.
- (4) Huynh, W. U.; Dittmer, J. J.; Alivisatos, A. P. *Science* **2002**, *295*, 2425.
- (5) Murphy, C. J.; Jana, N. R. *Adv. Mater.* **2002**, *14*, 80.
- (6) Wilson, O.; Wilson, G. J.; Mulvaney, P. *Adv. Mater.* **2002**, *14*, 1000.
- (7) Favier, F.; Walter, E.; Zach, M. P.; Benter, T.; Penner, R. M. *Science* **2001**, *293*, 2227.
- (8) Maier, S. A.; Kik, P. G.; Atwater, H. A.; Meltzer, S.; Harel, E.; Koel, B. E.; Requicha, A. A. G. *Nat. Mater.* **2003**, *2*, 229.
- (9) Jana, N. R.; Gearheart, L.; Murphy, C. J. *Chem. Commun.* **2001**, 617.
- (10) Jana, N. R.; Gearheart, L.; Murphy, C. J. *J. Phys. Chem. B* **2001**, *105*, 4065.
- (11) Jana, N. R.; Gearheart, L.; Murphy, C. J. *Adv. Mater.* **2001**, *13*, 1389.
- (12) Busbee, B. D.; Obare, S. O.; Murphy, C. J. *Adv. Mater.* **2003**, *15*, 414.
- (13) Johnson, C. J.; Dujardin, E.; Davis, S. A.; Murphy, C. J.; Mann, S. *J. Mater. Chem.* **2002**, *12*, 1765.
- (14) Gates, B.; Yin, Y.; Xia, Y. *J. Am. Chem. Soc.* **2000**, *122*, 12582.
- (15) Otten, C. J.; Lourie, O. R.; Yu, M. F.; Cowley, J. M.; Dyer, M. J.; Ruoff, R. S.; Buhro, W. E. *J. Am. Chem. Soc.* **2002**, *124*, 4564.
- (16) Yu, Y.-Y.; Chang, S.-S.; Lee, C.-L.; Wang, C. R. *J. Phys. Chem. B* **1997**, *101*, 6661.
- (17) Torigoe, K.; Esumi, K. *Langmuir* **1992**, *8*, 59.
- (18) Tierney, M. J.; Martin, C. R. *J. Phys. Chem.* **1989**, *93*, 2878.
- (19) Nikoobakht, B.; El-Sayed, M. A. *Langmuir* **2001**, *17*, 6368.

Table 1. Surfactants Used in This Paper^a

name	structure	abbreviation
decyltrimethylammonium bromide	$\text{CH}_3(\text{CH}_2)_9\text{N}(\text{CH}_3)_3^+ \text{Br}^-$	C ₁₀ TAB
dodecyltrimethylammonium bromide	$\text{CH}_3(\text{CH}_2)_{11}\text{N}(\text{CH}_3)_3^+ \text{Br}^-$	C ₁₂ TAB
myristyltrimethylammonium bromide	$\text{CH}_3(\text{CH}_2)_{13}\text{N}(\text{CH}_3)_3^+ \text{Br}^-$	C ₁₄ TAB
cetyltrimethylammonium bromide	$\text{CH}_3(\text{CH}_2)_{15}\text{N}(\text{CH}_3)_3^+ \text{Br}^-$	C ₁₆ TAB
octadecyltrimethylammonium bromide	$\text{CH}_3(\text{CH}_2)_{17}\text{N}(\text{CH}_3)_3^+ \text{Br}^-$	C ₁₈ TAB
cetylpyridinium chloride monohydrate	$\text{CH}_3(\text{CH}_2)_{15}(\text{C}_5\text{H}_5\text{N})^+ \text{Cl}^- \cdot \text{H}_2\text{O}$	C ₁₆ PC

^aThe solubility of the surfactants in this table is 0.1 M in water, with the exception of C₁₈TAB, which is 0.005 M.

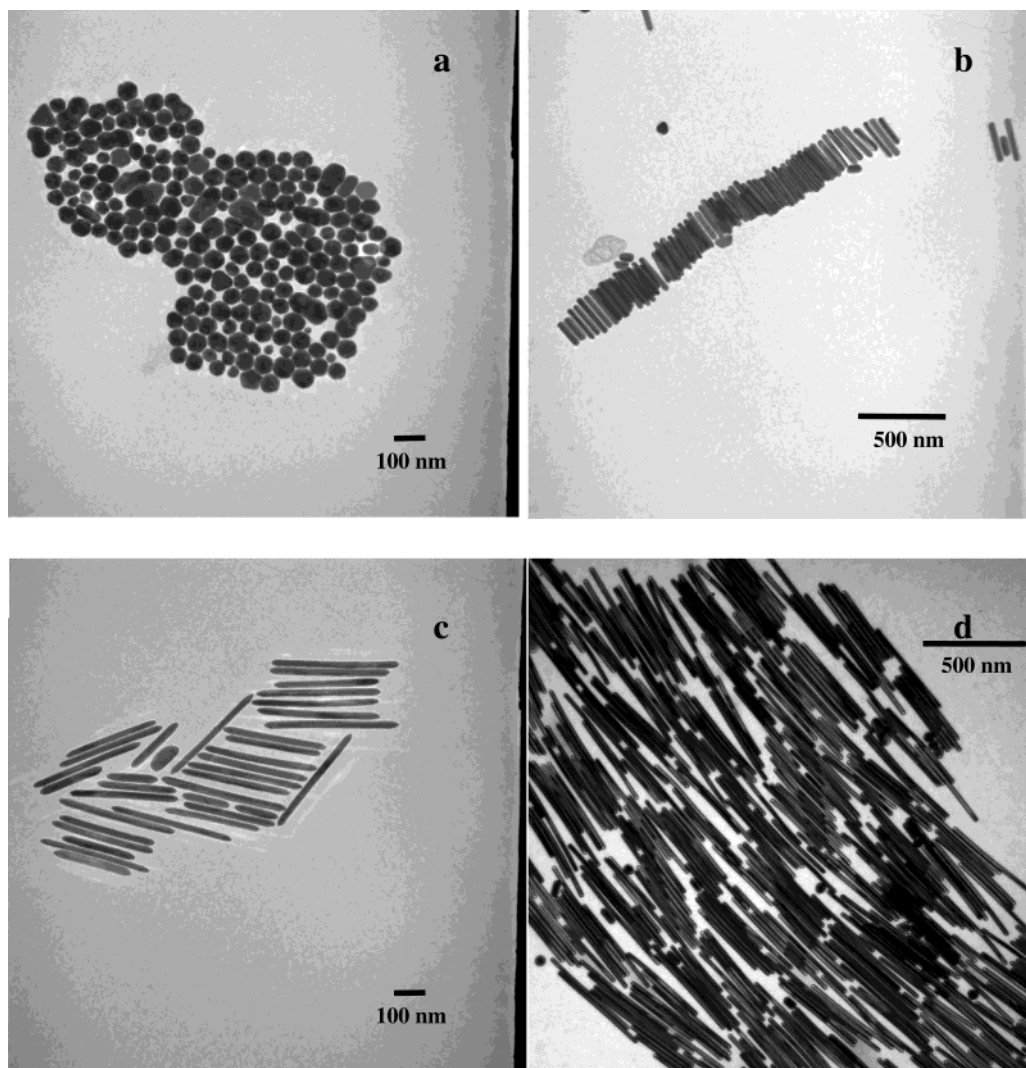


Figure 1. TEM micrographs of gold nanoparticles prepared in the presence of (a) C₁₀TAB, (b) C₁₂TAB, (c) C₁₄TAB, and (d) C₁₆TAB according to the procedures described in the Experimental Section, after purification to remove the spheres. Scale bars are 500 nm (b and d) and 100 nm (a and c).

to room temperature, and used within 6 h. Stock solutions of sodium borohydride and L-ascorbic acid in water were freshly prepared every time; other stock solutions are stable for up to 6 months. Purified deionized water (Continental Water Systems) was used for all reactions. All glassware was washed sequentially with aqua regia, tap water, and purified deionized water.

Instrumentation. Electronic absorption spectra were acquired with a Cary 500 UV–visible–near-IR spectrophotometer. Transmission electron microscopy (TEM) was performed with a Hitachi H-8000 transmission electron microscope with an accelerating voltage of 200 kV. TEM grids were prepared by placing 1 μL of the gold nanoparticle solution on a carbon-coated copper grid and allowing the solvent to evaporate at room temperature.

Preparation of the Gold Seed. The procedure that yields spherical gold nanoparticles 4 nm in diameter has been described by us.¹⁰ Briefly, a 20-mL aqueous solution containing 18.4 mL of deionized water, 0.5 mL of an aqueous 0.01 M HAuCl₄·3H₂O solution, and 0.5 mL of an aqueous 0.01 M trisodium citrate

solution was prepared in a conical flask. Next, 0.6 mL of an ice-cold aqueous 0.1 M NaBH₄ solution was added all at once with stirring. The solution turned pink immediately after the addition of the borohydride, indicating gold nanoparticle formation. This seed solution was used between 3 and 10 h after its preparation; 3 h is needed for any remaining borohydride to degrade by reaction with water, but longer than 10 h results in extensive aggregation of the gold particles, observable as a thin film at the water surface. In general, the seed solution was used 3 h after its preparation.

Preparation of Gold Nanoparticles of Various Aspect Ratios. A three-step seeding method developed by us was used.¹⁰ Three 15-mL plastic centrifuge tubes were labeled A, B, and C. Into each tube was placed 9 mL of “growth” solution; the growth solution consisted of 2.5×10^{-4} M HAuCl₄·3H₂O and 0.1 M surfactant in water (except for C₁₈TAB, which is only soluble to the extent of 0.005 M). Upon mixing of the gold(III) salt and surfactant, the solution changed color from light yellow to darker yellow, which can be taken as an indication of the formation of

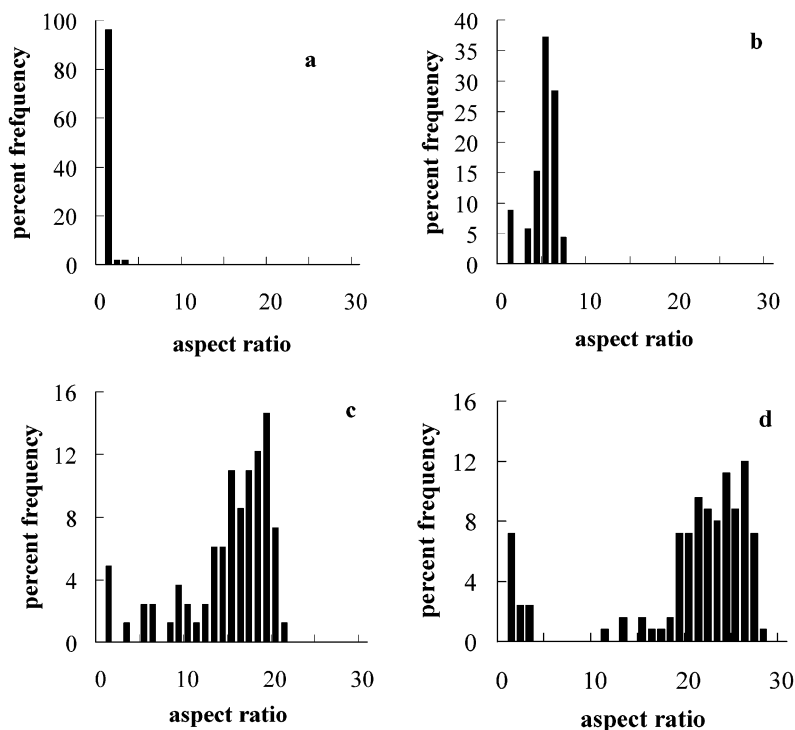


Figure 2. Histograms, based on the TEM images in Figure 1, that show the distribution of the gold nanoparticle aspect ratio as a function of the surfactant for (a) C_{10} TAB, (b) C_{12} TAB, (c) C_{14} TAB, and (d) C_{16} TAB.

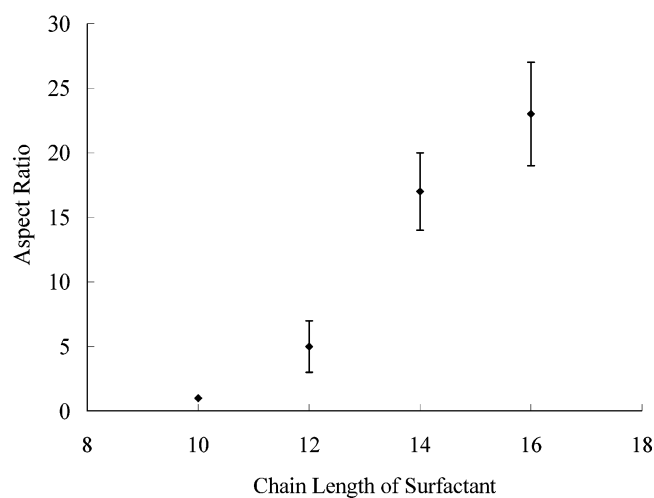


Figure 3. Plot of the aspect ratio of gold nanorods produced versus the number of carbon atoms in the surfactant's tail.

the complex ion $C_nTA^+ AuCl_4^-$.²⁰ Then, to each tube containing 9 mL of the growth solution was added 0.05 mL of a freshly prepared aqueous 0.1 M solution of ascorbic acid. The tubes were inverted 3 times to mix, and the resulting solution changed color from yellow to colorless, suggesting reduction of Au(III) to the Au(I) species. Next, 1.0 mL of the gold seed solution prepared in the previous section was added to tube A, and the tube was inverted 10 times to mix. After 30 s, 1.0 mL of the tube A solution was withdrawn and added to tube B. Tube B was inverted 10 times to mix. After 60 s, 1.0 mL of the tube B solution was withdrawn and added to tube C. Tube C was inverted 10 times to mix. Within 10 min, the color of the solution in tube C turned from colorless to various shades of pink-purple, depending on aspect ratio of the resulting gold nanoparticles. The solution in tube C was allowed to sit overnight to ensure full growth of the gold nanorods. The remaining solution in tube A turned red within 3 min, while the remaining solution in tube B turned red within 5 min, indicating metallic gold nanoparticles in each.

Shape Separation. Gold nanoparticles were concentrated and separated from the small nanospheres and surfactant by centrifugation. A total of 10 mL of the nanoparticle solution from tube C was centrifuged at 2000 rpm for 6 min. The red supernatant, containing mostly small gold nanospheres (diameters less than 20 nm), was drawn off with a syringe. The pink solid, containing nanorods and some platelets, was redispersed in 1 mL of deionized water and centrifuged at 2000 rpm for 6 min, 3 times, until most of the surfactant had been removed (no bubbles were observed upon shaking the tube).

Results and Discussion

Previous work by Nikoobakht and El-Sayed has shown that C_{16} TAB adsorbs in bilayers on gold nanorods, with the trimethylammonium headgroup of one monolayer facing the gold surface and the other facing the solvent to maintain water solubility.¹⁹ High-resolution TEM and electron diffraction data on our gold nanorods showed that the {111} face of gold is the surface at the ends of the nanorods (which exist as pentahedral twins), while the gold {100} face is the surface plane on the long axis of the nanorods.¹³ We postulated that the large headgroup size of the C_{16} TAB surfactant preferred the larger gold-atom spacing on the sides rather than at the ends of the nanorods; the {111} face of gold is the most close-packed and stable face. In principle, then, many simple trimethylammonium salts could be used to stabilize gold nanorod formation in water. In this paper, we examined a family of surfactants, which contain the same headgroup and counterion as C_{16} TAB but different alkyl chain lengths, and also we examined one surfactant that retained the 16-carbon chain but had a different headgroup and counterion (Table 1) as directing agents for the growth of gold nanorods according to the protocol established for C_{16} TAB.

Figure 1 shows TEM images of gold nanoparticles made according to the three-step seeding growth method described in the Experimental Section, after the separation of the spheres, as a function of the different surfactant chain lengths for C_n TAB ($n = 10, 12, 14, 16$). We note that,

(20) Kameo, A.; Suzuki, A.; Torigoe, K.; Esumi, K. *J. Colloid Interface Sci.* **2001**, *241*, 289.

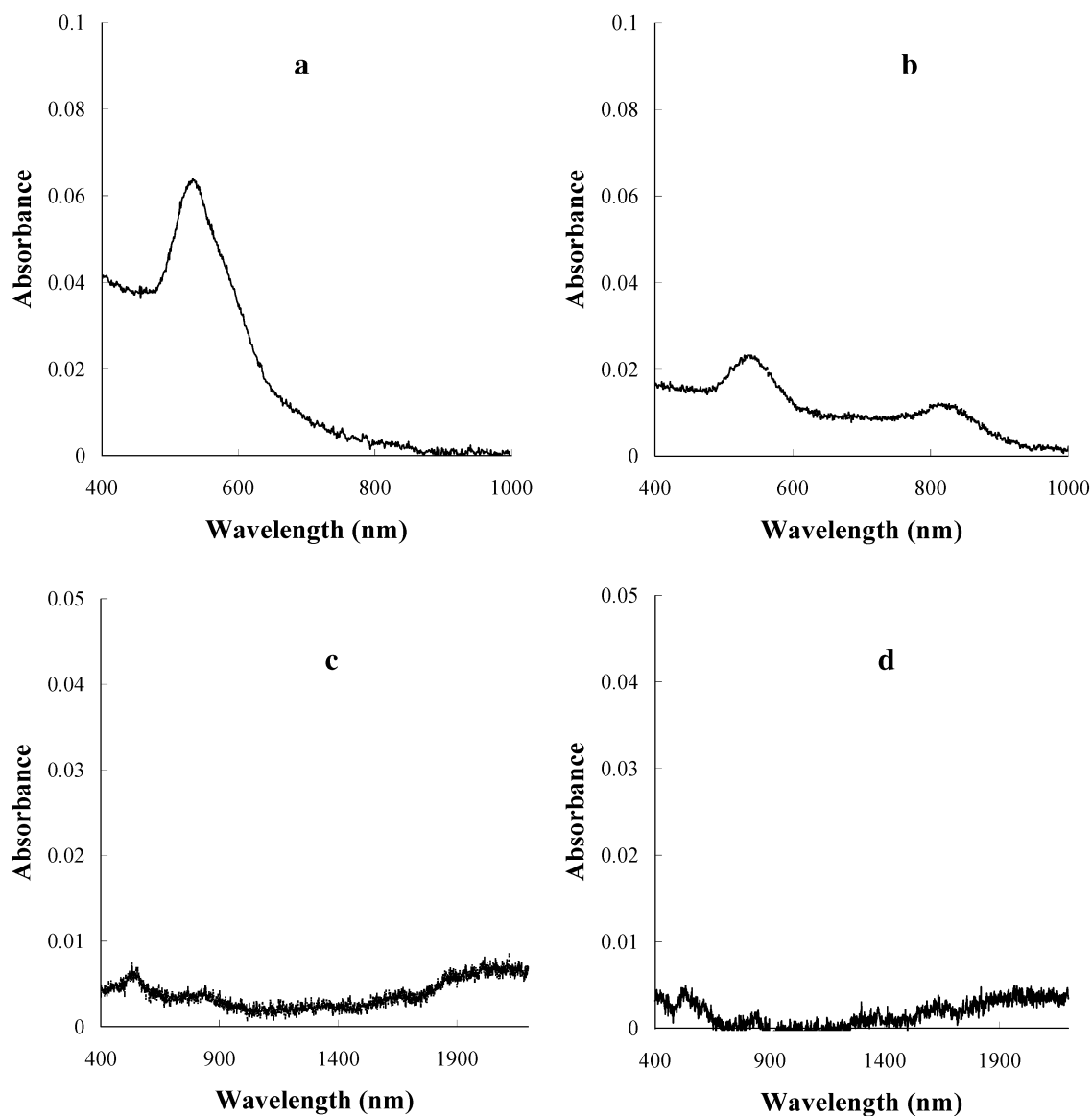


Figure 4. Electronic absorption spectra of gold nanoparticles prepared in the presence of (a) C_{10} TAB, (b) C_{12} TAB, (c) C_{14} TAB, and (d) C_{16} TAB.

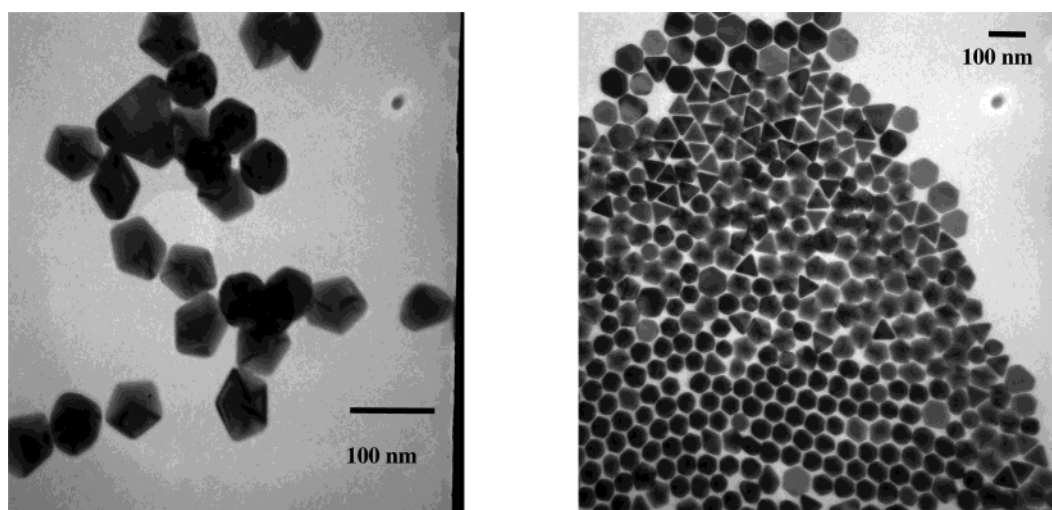


Figure 5. TEM micrographs of gold nanoparticles made in the presence of C_{16} PC, according to the same protocol that produces aspect ratio 23 nanorods if C_{16} TAB is used. Scale bars are 100 nm.

for all surfactants, ~80% of the nanoparticle products are spheres, with no clear trend following the surfactant chain

length, although it is easier to separate rods from spheres for higher aspect ratio rods. Clearly, the trimethylam-

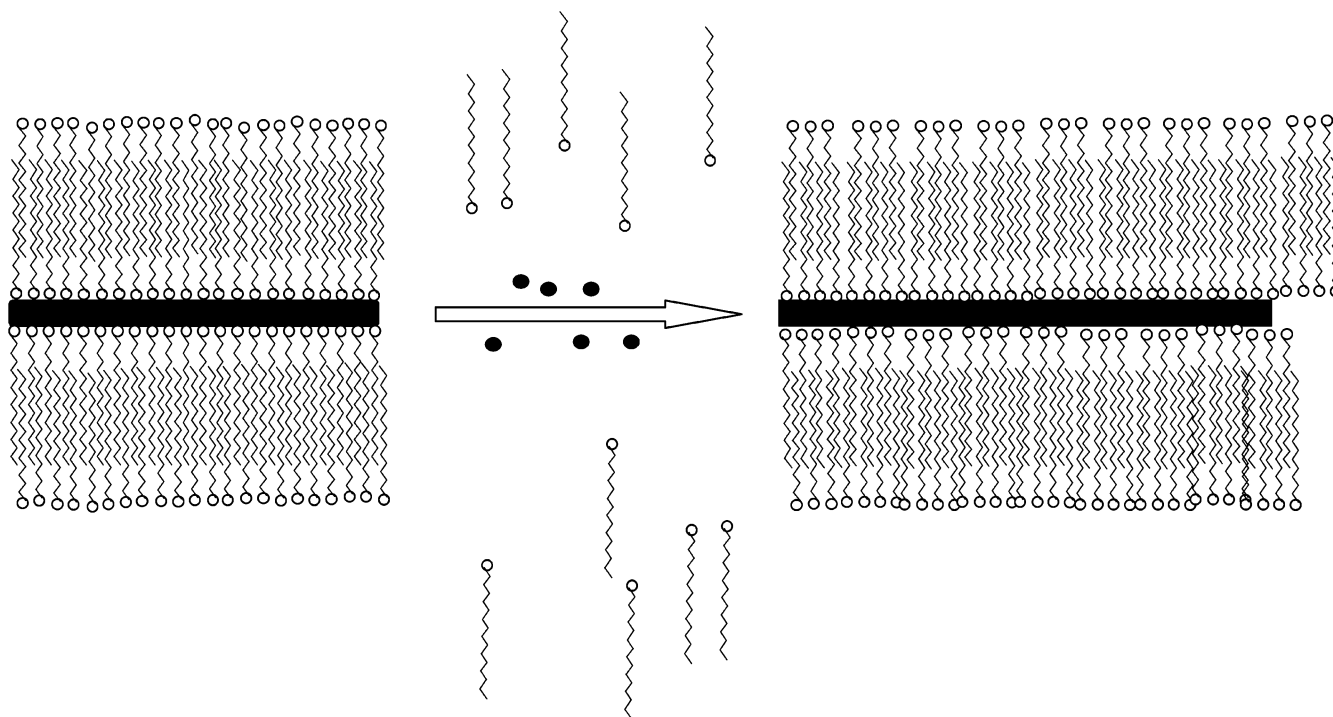


Figure 6. Cartoon illustrating “zipping”: the formation of the bilayer of C_n TAB (squiggles) on the nanorod (black rectangle) surface may assist nanorod formation as more gold ions (black dots) are introduced.

monium headgroup alone is not sufficient to direct nanoparticle growth into rods, or all of the surfactants would have yielded nanorods. The general trend is that, as the length of the alkyl chain is increased, higher-aspect-ratio nanorods can be obtained. Figure 2 shows histograms of the nanoparticle aspect ratio that correspond to the TEM images of Figure 1.

For C_{10} TAB, 96% of the gold nanoparticles were spherical (aspect ratio 1) and only 4% were short rods (aspect ratio 2–3), even after centrifugation to remove nominal nanospheres. No higher aspect ratio nanorods were found in samples in which ~ 400 nanorods at a minimum were counted. For C_{12} TAB, after separation from the spheres, 92% of the nanoparticles were low-aspect-ratio (5 ± 2) nanorods, with 8% of the nanospheres remaining (it becomes easier to separate the nanorods from the spheres the longer the nanorods are). For C_{14} TAB, the aspect ratio of the resulting gold nanorods after separation from the spheres was 17 ± 3 , with an additional 22% of the particles counted having lower aspect ratios (5–13). For C_{16} TAB, the surfactant we had used previously to control the gold nanorod aspect ratio up to ~ 20 ,¹³ the data are consistent with what we had before for the longest rods possible with an aspect ratio of 23 ± 4 . C_{18} TAB was also used as a directing agent, but because its solubility in water is only 5% of the other surfactants, it is problematic to directly compare the results. In the case of C_{18} TAB, a few nanorods of medium (~ 10) aspect ratio were obtained, but other irregular shapes dominated the nanoparticle size distribution. In the case of C_n TAB for $n = 10$ –16, the nanoparticle width was constant (25 ± 2 nm) and the length of the longest nanorods increased with surfactant alkyl chain length (Figure 3). We note that another paper in the literature reports the same general phenomenon that we observe: gold nanoparticles made photochemically in the presence of $C_nTA^+Cl^-$ show higher aspect ratio materials for larger n .²⁰

Electronic absorption spectra were acquired for gold nanoparticles of varying aspect ratios (Figure 4). For gold nanospheres, as in the case for C_{10} TAB, the plasmon band

appears at 528 nm, as expected. Higher aspect ratio nanoparticles show both transverse and longitudinal plasmon bands,^{2,5,6,10,18} and the longitudinal band moves into the near-IR region the longer the nanorods are. In our samples, the transverse plasmon band, corresponding to the absorption/scattering of light along the short axis of the nanoparticles, was still ~ 520 nm, slightly blue-shifting for increasing aspect ratio in accord with others;² the longitudinal plasmon band, corresponding to the absorption/scattering of light along the long axis of the nanoparticles, moved from 820 nm (for aspect ratio 5 ± 2 gold nanorods made with C_{12} TAB) to ~ 1800 – 2200 nm (broad, for aspect ratio 17 ± 3 gold nanorods made with C_{14} TAB) and beyond 2200 nm for aspect ratio 23 ± 4 gold nanorods made with C_{16} TAB. These samples were extensively purified to yield “pure nanorod” spectra with no contribution from the spheres; during the course of the separation, however, many rods are lost, and so the spectra for the high aspect ratio rods are for very dilute solutions that slowly precipitate out over time.

We also examined the surfactant cetylpyridinium chloride, $C_{16}PC$, as a directing agent for gold nanorod growth. In this molecule, the cetylpyridinium headgroup is larger and more anisotropic in shape compared to the alkyltrimethylammonium headgroup of the other surfactants. The counterion is also different. The synthetic procedure to make gold nanoparticles using $C_{16}PC$ produced no nanorods whatsoever (Figure 5). Instead, in addition to gold nanospheres, triangles, pentagons, and hexagons were observed, in roughly equal proportions and of similar widths, likely corresponding in three dimensions to tetrahedra, dodecahedra, and icosahedra of gold.

What is the mechanism of growth control in these nanomaterial syntheses? Our previous work with C_{16} TAB and gold nanorods suggested that, during nanorod growth, preferential adsorption of C_{16} TAB to the different crystal faces of gold led to the inhibition of growth along the long axis of the rods and, therefore, enhanced growth at the

ends of the nanorods.^{13,21} We postulated at that time that C₁₆TAB bilayer formation would also encourage this anisotropic growth^{13,19} in that C₁₆TAB molecules might have a preference for the side face of the rods via their headgroups and their tails would have a preference to interact with each other via van der Waals interactions. These ideas are in general born out by the experiments presented here: one would predict that the longer the tail length, the more stable the bilayer. What perhaps is surprising is that the tail–tail interactions we postulate seem to be more important than the headgroup interactions with the gold surface (because C₁₀TAB yields practically no rods of even a modest aspect ratio).

C_{*n*}TAB for *n* = 10, 12, 14, and 16 are all well-known to form micelles in aqueous solution.²² The critical micelle concentration decreases from mM for *n* = 10 to 10 μM for *n* = 16 logarithmically with the carbon number in the tail.²² Because our synthetic conditions are 0.1 M surfactant, but with many more ions in solution, it is not clear if the surfactants are forming micelles to the same extent that they are in plain water. Nonetheless, using data from the micelle literature, we can estimate the degree to which the hydrocarbon chain stabilizes bilayer formation. The hydrocarbon contribution to the standard free energy of micellization for C_{*n*}TAB in water, following a mass-action model that uses empirical data, has been estimated to be²²

$$\Delta G^\circ = 2.303(2 - zj)RT(0.1128 - 0.3074n) \quad (1)$$

where *n* is the number of carbon atoms in the surfactant tail, *z* is the charge on the micelle, *j* is the aggregation number of the micelle, *j* − *z* then corresponds to the number of anions strongly bound to the micelle, *R* is the gas constant, and *T* is the temperature. If we assume for the sake of estimation that *z* and *j* do not change upon bilayer

formation on gold nanorods for the different surfactants and that the *z*/*j* ratio is significantly smaller than 1 because of strongly bound counterions, then we estimate that $\Delta G^\circ_{n=10} = -29.6$ kJ/mol, $\Delta G^\circ_{n=12} = -35.8$ kJ/mol, $\Delta G^\circ_{n=14} = -41.9$ kJ/mol, and $\Delta G^\circ_{n=16} = -48.1$ kJ/mol. The differences between the surfactants, then, are ~6 kJ/mol per two methylene units, which is significant compared to *RT* (~2.5 kJ/mol). Thus, the dynamic formation of a bilayer of the surfactant on gold surfaces in a “zipping” manner via the hydrocarbon tails may indeed provide enough stabilization during gold nanorod growth to promote the formation of longer nanorods for more stable bilayers (Figure 6). Clearly, however, a long hydrocarbon chain in the directing surfactant is not sufficient to guarantee gold nanorods (cf. the case of C₁₆PC). We can imagine the nanorod growth mechanism, then, to include the trimethylammonium surfactant headgroup providing preferential binding to different gold faces, with simultaneous van der Waals interactions of adjacent surfactant tails “zipping” up the long axis of the gold nanorod.

Conclusions

We demonstrated in previous work that gold nanorods of a controlled aspect ratio can be made in aqueous solution using C₁₆TAB as the directing agent.¹⁰ In this paper, we examined C_{*n*}TAB analogues in which the length of the hydrocarbon tail was varied, keeping the headgroup and counterion constant, and also an example in which the tail length was kept the same but the headgroup and counterion both varied. We found that the length of the surfactant tail is critical for producing gold nanorods, with longer chain lengths supporting longer gold nanorods. We propose a “zipping” mechanism to account for our results in which the van der Waals stabilization of the surfactant bilayer on the gold surface due to interchain packing assists the underlying nanorod formation.

Acknowledgment. We thank the National Science Foundation for funding.

LA034919I

(21) Murphy, C. J. *Science* **2002**, *298*, 2139.

(22) Anacker, E. W. In *Cationic Surfactants*; Jungermann, E., Ed.; Marcel Dekker: New York, 1970.